Characterization of nonlinear carrier dynamics in silicon strip nanowaveguides

Ivan Aldaya and Paulo Dainese
"Gleb Wataghin" Physics Institute
State University of Campinas, Brazil
Email: dainese@ifi.unicamp.br

Andrés Gil-Molina and Julián L. Pita
School of Electrical and
Computing Engineering
State University of Campinas, Brazil

Hugo L. Fragnito
MackGraphe - Graphene and
Nanomaterials Research Center
Mackenzie Presbyterian University, Brazil

***Abstract*—Nonlinear carrier recombination dynamics is characterized in a 450 nm × 220 nm silicon nanowire by employing a time-resolved pump-and-probe experiment. Our results show that the recombination rate is faster at the early stages of the decay as compared to the final stages, in agreement with trap-assisted mechanism. We have also demonstrated that by operating at high carrier density, faster excess carrier generation and recombination can be obtained, which we have used to improve the speed of an all-optical FCA based silicon switch from about 7 to 1 ns.**

***Index Terms*—silicon photonics, free carriers, lifetime.**

I. Introduction

Free-carriers generated via two-photon absorption (TPA) have been identified as an important mechanism affecting the performance of both active and passive silicon photonic devices [5], [1], [2], [3], [4]. The dispersion and absorption in waveguides and cavities are both modified in the presence of excess electron-hole pairs within the silicon core region. These phenomena are referred respectively as FCD (Free-Carrier Dispersion) and FCA (Free-Carrier Absorption) [5]. The design of state-of-the-art devices hence relies on an accurate characterization of the carrier density dynamics, which in turn depends on generation, diffusion, and recombination rates. Generation through TPA is generally assumed instantaneous for telecommunication applications. The time scale involved in spatial diffusion depends on the waveguide cross-section dimensions, and has been extensively modeled in photonic crystal cavities [6] as well as in rib waveguide structures [7]. A key aspect in rib or photonic crystal cavities is that diffusion pushes the free-carriers away from the optical mode region. As a consequence, FCD and FCA decrease over time, not only because of recombination but also due to diffusion. In silicon nanowires (or strip waveguides), the silicon core is surrounded by a dielectric material (such as silicon oxide), and therefore the excess carriers no longer leave the modal region. As a result, carrier recombination processes determine the rate at which free-carriers cease to impact the optical mode.

In most communication applications, carrier recombination is treated as a time decay exponential process, generally characterized by a single lifetime [5]. In silicon, band-to-band radiative recombination is generally neglected due to its indirect bandgap, and the main mechanisms are Auger and trap-assisted recombination, the later being dominant as long as the carrier densities do not significantly exceed about 10^{19} cm^{-3} [9]. Although the single-exponential decay is justified under certain conditions (i.e. minority-dominated carrier lifetime), it is well known that strictly speaking, recombination processes are not single-exponential [10]. In this paper, we studied the recombination of carriers in a silicon nanowaveguide, under conditions that allow clear observation of non-exponential decay. Using a pump and probe technique, we characterized the carrier dynamics for different pump power. The results demonstrate a reduction in the decay lifetime by operating at high injection level, which may be engineered to create faster all-optical modulators.

II. Experimental setup and methods

The sample that we analyzed in this work is a silicon on insulator (SOI) strip waveguide with a cross-section of 450 nm×220 nm and a length of 5.9 mm. The sample had silicon oxide cladding and light was coupled in and out using grating couplers. The coupling and transmission losses were calculated by means of linear regression of samples with three different lengths (2.4, 5.9, and 30 mm), and the values obtained were 3.1 dB per grating and 1.4 dB/cm, respectively.

Figure 1a shows the setup of the pump-and-probe experiment employed to characterize the free-carrier recombination dynamics of the waveguide under test. The pulsed pump was synthesized by externally modulating a continuous wave laser (operating at 1547 nm) with a Mach-Zehnder electro-optical modulator (EOM) driven by an electrical signal with a 500 kHz repetition rate and a pulse duration of 130 ps or 20 ns. The employed EOM had a bandwidth of 20 GHz and an extinction ratio >30 dB. The pulsed signal was then boosted by an erbium-doped fiber amplifier (EDFA). In order to avoid undesired carrier generation, the bias voltage of the EOM was set for maximum peak pump power at the output of the EDFA that ensures minimal continuous-wave component after the EOM. In addition, free-carrier generation through TPA induced by amplified spontaneous emission (ASE) is prevented by the use of an optical bandpass filter (BPF) that removes the out-of-band noise and by an acousto-optic modulator (AOM) operating as an optical gate. The used AOM has a relatively slow response, falling and rising times around 10 ns, however, it was chosen because of its high extinction ratio, 50 dB, which allowed us to suppress the ASE noise that would be present

978-1-5090-6241-6/17/$31.00

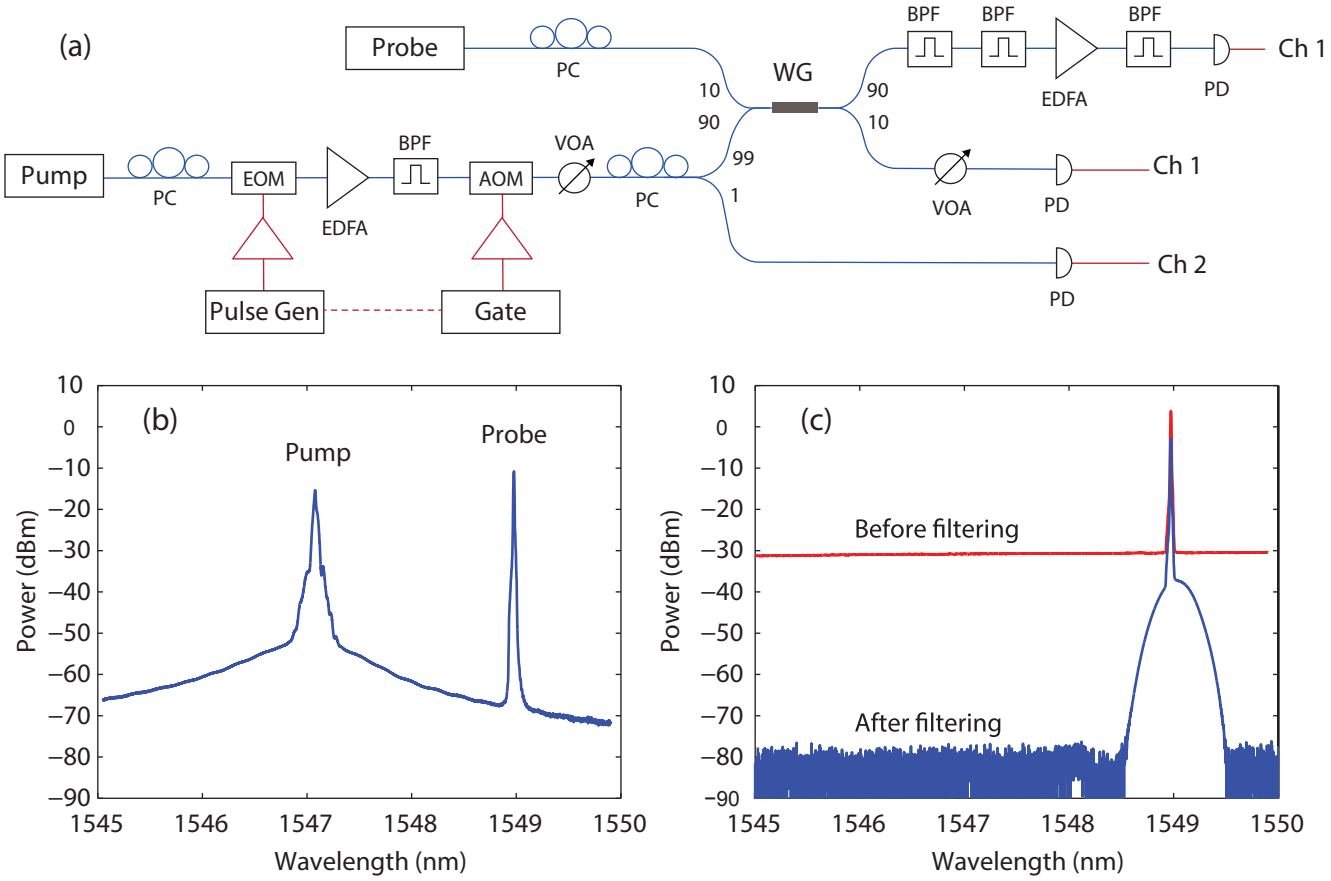

Fig. 1. (a) Experimental setup employed to characterize the free-carrier lifetime in SOI strip waveguides. PC: polarization controller; EOM: electro-optical modulator, EDFA: erbium-doped fiber amplifier; BPF: bandpass filter; AOM: acousto-optic modulator; VOA: variable optical attenuator; PD: photodetector; and WG: waveguide under test.(b) Power spectrum at the input of WG. (c) Power spectrum before and after the last BPF.

between pulses. It is worth noting that the synchronization between the pulse and the gating was achieved by using a common clock signal. The power of the pump signal was then controlled using a variable optical attenuator (VOA). Part of the pump signal, 1%, was derived to monitor the pulse shape as well as the input power level. Before being launched into the waveguide, the pump was combined in a 10-90 optical coupler with the probe, a continuous wave laser emitting at 1549 nm. The spectrum of the combined signal is shown in Figure 1b, where the low noise level can be appreciated. Since the coupling was performed through grating couplers designed for quasi-tranverse electric (TE) operation, the states of polarization of both the pump and the probe were optimized using independent polarization controllers (PCs).

At the output of the waveguide, an additional 10-90 splitter was used to divide the signal. The 10% output was employed to measure the insertion loss in the waveguide, whereas the 90% output was filtered out using two cascaded BPFs to block the pump. Given its low power, the probe was amplified using a pre-EDFA, whose output was filtered to eliminate the out-of-band ASE as can be seen in Figure 1c. A two-channel oscilloscope was used to capture the signals. The input to Channel 1 (an optical input with an in-built 28 GHz photodetector, PD) was switched to measure either the filtered probe signal or the output pulse, whereas in Channel 2 (electrical input), the output of an external photodetector was captured in order to monitor the pump signal. The capturing window was set to 200 ns, where 6300 points were taken, each one corresponding to an ensemble average of 64 samples.

III. Results and Discussion

The ratio between the detected output probe signals for pump off and pump on was used to obtain the total nonlinear loss in the waveguide (excluding therefore linear losses). Figure 2a shows an example where two different regimes can be clearly identified: an initial peak due to non-degenerate TPA, followed by a slower stage where free-carrier absorption is the dominant nonlinear loss mechanism. For waveguides with larger cross sections, an intermediate stage where diffusion impacts the decay rate has been reported [7]. In our case, however, the dimensions of the waveguide cross-section result in diffusion times on the order of a few ps, which is too short to be identified in our measurement. We focused on the FCA-

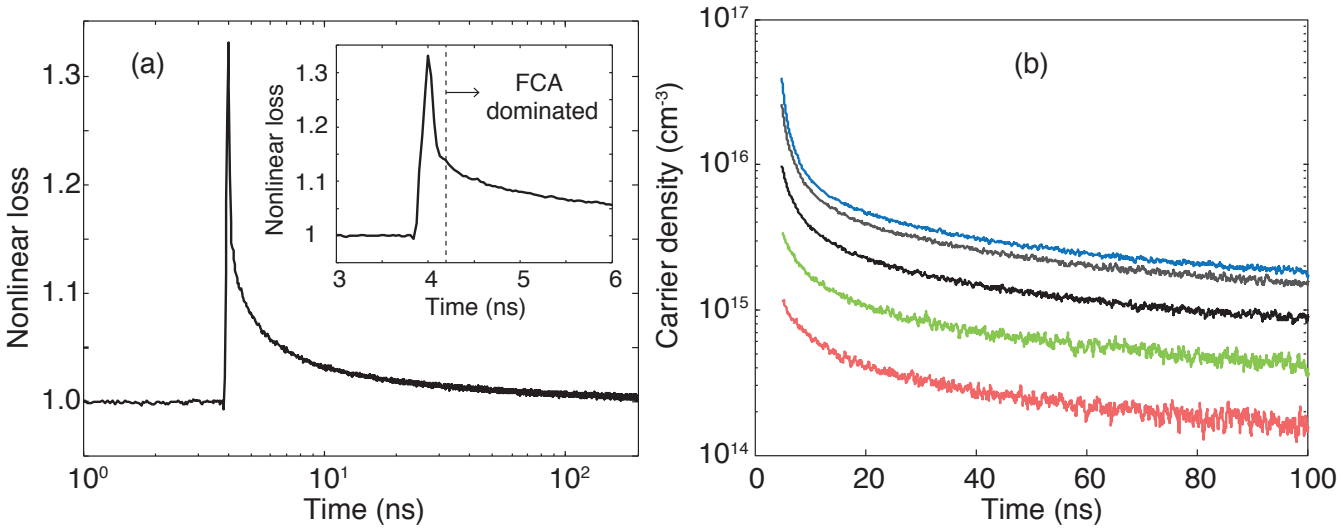

Fig. 2. Analysis of carrier density dynamics using 130-ps pump pulses. (a) Nonlinear loss as a function of time for 0.28 W pump power; The inset shows a zoom of the normalized nonlinear loss around the pump pulse in linear time scale; (b) carrier density as a function of time for for different pump peak powers (0.07, 0.14, 0.28, 0.56, and 1.1 W).

dominated stage, in which the carrier density can be extracted from the accumulated nonlinear loss along the waveguide:

$$L_{FCA}(t) = \exp\left[\sigma_a \int_0^L N(z,t)\cdot dz\right], \qquad (1)$$

where σ_a is the FCA absorption cross-section ($1.45{\cdot}10^{-21}$ cm^2 at 1550 nm [5]), N is the carrier density, z is the longitudinal coordinate, and L is the length of the waveguide. The previous expression can be re-written in terms of the average carrier density along the waveguide ($\bar{N}$) as $L_{FCA} = \exp[\sigma_a \bar{N}(t) L]$. For the length and pump input power considered in our experiment, the carrier density does not deplete significantly over the waveguide and therefore the average density is not significantly different from the actual density. Using the nonlinear loss curve beyond 5 ns (see inset in Figure 2a), we ensure that only FCA contributes to the nonlinear loss, and the time-resolved carrier density (averaged over the waveguide length) can be estimated as:

$$\bar{N}(t) = \frac{\ln\left[L_{FCA}(t)\right]}{\sigma_a L}. \qquad (2)$$

Figure 2b shows the calculated carrier density, the curve in black corresponding to the data from Figure 2a. Clearly, the decay does not follow a simple exponential (as the decay curve is not a straight line in logarithmic scale). In addition, from this curves, we can observe that the instantaneous lifetime, defined as $-\bar{N}/(d\bar{N}/dt)$, is faster in the beginning, when the carrier density is higher, and get slower at the later stages of recombination. In order to explore the dynamics as a function of the excess carrier density, we took measurements for different pump power levels, from 0.07 W to 1.1 W. The obtained results are also shown in Figure 2b. A nonlinear decay behavior is observed in all curves. We can notice, however, that at the time scale of this measurements, the curves corresponding to higher pump power, and therefore higher initial carrier density, decay faster at the early stages can be observed when compared to the lower pump power curves.

The nonlinear dynamics observed in these results might be useful to engineer faster all-optical switching. As the FCA contribution to nonlinear loss depends exponentially on the carrier density times interaction length, it is interesting to evaluate how long it takes for the carrier density to drop from its initial value. This point can be seen more directly in Figure 3a, in which we have plotted the normalized carrier density, i.e., each curve in Figure 2b was divided by its maximum density value. By controlling the device length, one could, in principle control the amount of nonlinear loss somewhat independently form the initial density value (limited however by linear loss and TPA at the pump wavelength). As can be seen, the curves corresponding to higher pump power, and thus higher initial carrier density, decay faster than the lower power ones. This statement can be quantitatively assessed by measuring the time it takes to reach, for example, the half-maximum value. The highest density decays in less than 1 ns while for the lowest density, it takes about 7 ns. This nonlinear dynamics is in agreement with trap-assisted recombination [10]. Moreover, in the case of surface recombination, it is well known that the decay can be accelerated by reducing the waveguide dimension as well as by increasing the surface flaw density. This strategy, along with the results demonstrated in this paper, can be explored to create faster FCA based all-optical switching.

Once the carrier recombination dynamics was studied, we analyzed the nonlinear loss for a long pump pulse (20 ns), in order to quantify not only the decay rate but also the carrier build up dynamics. This would be important in an all-optical non-parametric optical switch, for example. Figure 3 shows the normalized nonlinear losses captured for various pump power levels ranging from 2 to 170 mW. As expected from

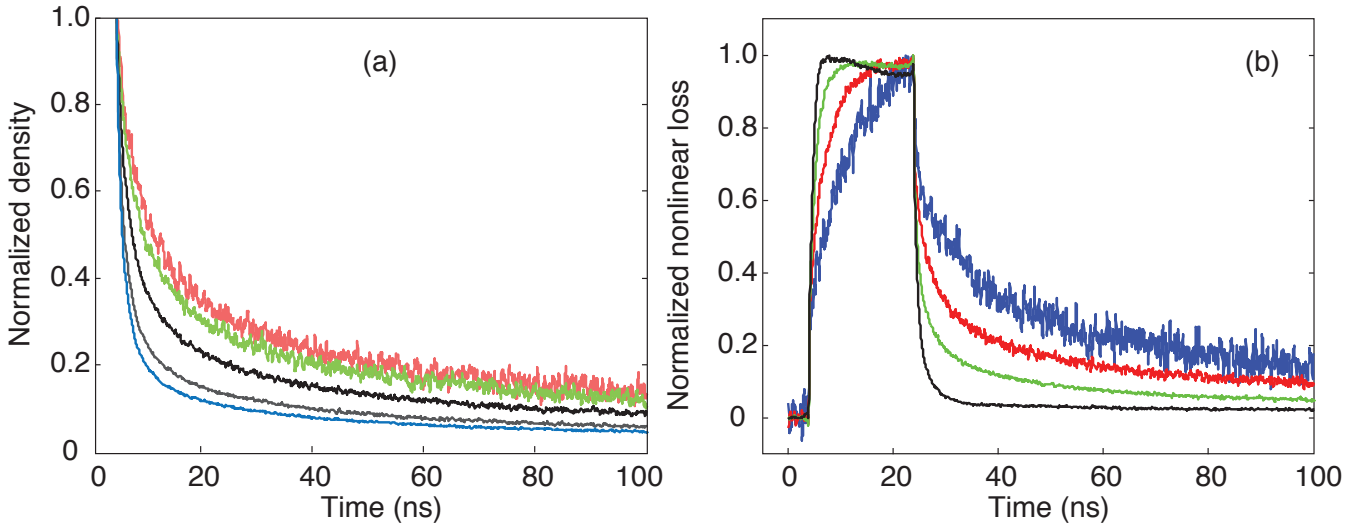

Fig. 3. (a) Normalized carrier density as a function of time when 130-ps pump pulses with power levels of 0.07, 0.14, 0.28, 0.56, and 1.1 W are used. (b) Normalized nonlinear loss as a function of time for 20-ns pump pulses at different pump power levels (2, 19, 75, and 170 mW).

the previous recombination time analysis, higher pump power results in a faster device, not only in the decay stage but also in the build up stage.

IV. Conclusions

In summary, carrier recombination dynamics in silicon strip nano-waveguides was studied using time-resolved FCA pump-and-probe measurements. Our results reveal a nonlinear carrier decay curve, with faster rates at the early decay stages as compared to final decay stages, a behavior consistent with trap-assisted recombination processes [10]. From a practical point of view, operating at elevated carrier densities, in our case higher than about 10^{15} cm^{-3}, results in accelerated dynamics. With long pump pulses, we have demonstrated improved performance on both generation as well as recombination. Our results might be useful to understanding complex dynamics in nonlinear waveguides and cavities where FCA and FCD play a major role, as well as potentially leading to faster all-optical switching.

Acknowledgements

This work was supported by FAPESP (13/20180-3, 15/11779-4, 12/50259-8, and 15/04113-0), CAPES, and CNPq (574017/2008-9).

References

[1] Johnson, Thomas J., Matthew Borselli, and Oskar Painter. "Self-induced optical modulation of the transmission through a high-Q silicon microdisk resonator." Optics Express 14.2, 817-831 (2006).
[2] A. Blanco-Redondo *et al.*, "Observation of soliton compression in silicon photonic crystals," Nat. Comm. **5**, 3160 (2014).
[3] F. Leo *et al.*, "Coherent supercontinuum generation in a silicon photonic wire in the telecommunication wavelength range," Opt. Lett. **40**, 1 (2014).
[4] L. Fan *et al.*, "An all-silicon passive optical diode," Science **335**, (2012).
[5] Q. Lin, O. Painter, and G. Agrawal, "Nonlinear optical phenomena in silicon waveguides: Modeling and applications," Opt. Express **15**, 16604–16644 (2007).
[6] T. Tanabe, H. Taniyama, and M. Notomi, "Carrier diffusion and recombination in photonic crystal nanocavity optical switches," J. of Lightwave Tech.26, **26**11, 1396-1403 (2008).
[7] Y. Liu and H. K. Tsang, "Time dependent density of free carriers generated by two photon absorption in silicon waveguides," App. Phys. Let. **90**, 211105 (2007).
[8] R. van Laer *et al.*, "Interaction between light and highly confined hypersound in a silicon photonic nanowire," Nature Photon. **9**, 199-203 (2015).
[9] S. Sze and K. Ng, *Physics of Semiconductor Devices*, 3rd Edition, Wiley (2006).
[10] J. S. Blakemore and Heinz K. Henisch, *Semiconductor Statistics*, Elsevier (1962).